Modular expression analysis reveals functional conservation between human Langerhans cells and mouse cross-priming dendritic cells

Maxim N. Artyomov,[1]* Adiel Munk,[1]* Laurent Gorvel,[1] Daniel Korenfeld,[1] Marina Cella,[1] Thomas Tung,[2] and Eynav Klechevsky[1]

[1]Department of Pathology and Immunology and [2]Department of Surgery/Plastic and Reconstructive Surgery Center, Washington University School of Medicine, St. Louis, MO 63110

Characterization of functionally distinct dendritic cell (DC) subsets in mice has fueled interest in whether analogous counterparts exist in humans. Transcriptional modules of coordinately expressed genes were used for defining shared functions between the species. Comparing modules derived from four human skin DC subsets and modules derived from the Immunological Genome Project database for all mouse DC subsets revealed that human Langerhans cells (LCs) and the mouse XCR1$^+$CD8α^+CD103$^+$ DCs shared the class I–mediated antigen processing and cross-presentation transcriptional modules that were not seen in mouse LCs. Furthermore, human LCs were enriched in a transcriptional signature specific to the blood cross-presenting CD141/BDCA-3$^+$ DCs, the proposed equivalent to mouse CD8α^+ DCs. Consistent with our analysis, LCs were highly adept at inducing primary CTL responses. Thus, our study suggests that the function of LCs may not be conserved between mouse and human and supports human LCs as an especially relevant therapeutic target.

CORRESPONDENCE
Eynav Klechevsky:
eklechevsky@path.wustl.edu

Abbreviations used: CTL, cytotoxic T cell; ILT, inhibitory immunoglobulin-like transcript; LC, Langerhans cell; mDC, myeloid DC; pDC, plasmacytoid DC.

DCs are a heterogeneous group of professional APCs. Upon activation, DCs migrate to secondary lymphoid organs and present antigen to their cognate T cells for the induction of adaptive immune responses (Banchereau and Steinman, 1998). In human cancer, there is now clinical evidence suggesting that the induction or activation of CD8$^+$ T cells can contribute to the arrest of tumor growth and increased patient survival. In principle, targeting tumor antigens to DCs may enhance protective CD8$^+$ T cell responses due to the ability of DCs to cross-present exogenous antigens (Segura and Villadangos, 2009). In cross-presentation, exogenous proteins are internalized, processed, and presented to CD8$^+$ T cells by MHC class I molecules. Specific DC populations (CD8α^+/CD103$^+$ DCs in the mouse, blood CD141$^+$ DCs in humans) are thought to be particularly adept in cross-presentation of antigens compared with others (Bachem et al., 2010; Jongbloed et al., 2010; Poulin et al., 2010; Romani et al., 2010).

Studies examining the DCs in the skin, the main targets of vaccines, showed that healthy human skin displays multiple DC populations: Langerhans cells (LCs) in the epidermis and interstitial DCs in the dermis consisting of CD1a$^+$ and CD14$^+$-expressing DCs (Lenz et al., 1993; Nestle et al., 1993; Klechevsky et al., 2008; Klechevsky, 2013). CD141 was recently reported to mark a population within the dermal CD1a$^{(dim)}$ DCs and is also known to be a marker expressed on dermal CD14$^+$ DCs (Chu et al., 2012; Haniffa et al., 2012). We, and others, have previously shown that human epidermal LCs are more efficient at priming naive CD8$^+$ T cells into potent cytotoxic T cells (CTLs) compared with the dermal CD14$^+$ DCs (Ratzinger et al., 2004; Klechevsky et al., 2008, 2009; Polak et al., 2012). Dermal CD14$^+$ DCs were later shown to induce regulatory T cells (Chu et al., 2012) and impaired priming of CTLs due to their IL-10 production and the expression of

*M.N. Artymov and A. Munk contributed equally to this paper.

The Rockefeller University Press $30.00
J. Exp. Med. 2015 Vol. 212 No. 5 743–757
www.jem.org/cgi/doi/10.1084/jem.20131675

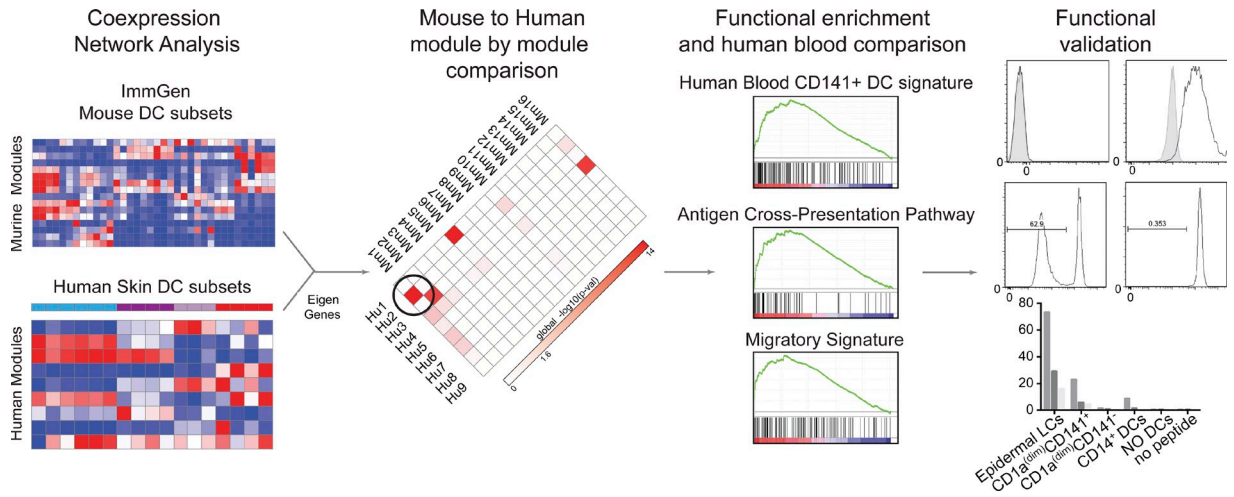

Figure 1. Experimental strategy. The research strategy showing the computational and functional analyses that are involved in identifying and validating functional homology between human and mouse DC subsets.

the inhibitory immunoglobulin-like transcript (ILT) receptors (Banchereau et al., 2012a,b).

Although cellular heterogeneity has been studied extensively in the immune system, understanding the biological functions of various DC subsets in humans is underdeveloped relative to the mouse. The alignment of DC subsets between mice and humans is of key importance in correlating human studies with mouse in vivo experiments. Transcriptional profiling is a powerful tool that has been used to examine several aspects of antigen presentation identity (Crozat et al., 2010b; Gautier et al., 2012). These and other studies used gene-centric, fold-change-based approaches to focus on the implications of expression differences between individual genes. More recent studies have integrated methods to harness the power of combining datasets and the coordinate expression of genes across cell types and species (Crozat et al., 2010b). These studies have helped identify pathways related to disease (Chaussabel et al., 2008; Berry et al., 2010), hematopoietic lineage differentiation (Ng et al., 2009; Novershtern et al., 2011) and T cell differentiation state (Doering et al., 2012).

In this study, we used a transcriptional profiling approach combined with network-based computational analysis and functional assays as a tool for investigating the functional similarities that might exist between human skin DCs and the mouse cross-presenting $CD8\alpha^+/CD103^+$ DC subsets.

RESULTS

Generation of coherent functional modules of co-expressed genes

Determining the homology between the murine and the human DC systems is an important unresolved issue, not only for the appropriate translation of mouse data for clinical use, but also to develop better preclinical models for human disease. One of the main controversies in the DC literature is the contribution of LCs in human versus mouse immunity (Romani et al., 2010). To reconcile the functional differences between mouse and human LCs, we performed a cross-species comparison using co-expression module analysis between human cutaneous DCs and mouse DCs (Fig. 1). This type of analysis groups genes together based on the similarity of their changes between subsets. We applied weighted gene co-expression network analysis (WGCNA) to define conserved transcriptional modules (Langfelder and Horvath, 2008). This computational approach is based on the idea that the probability for multiple transcripts to follow a complex pattern of expression across dozens of conditions only by chance is low. Thus, groups of genes that segregate together across many different conditions should constitute coherent and biologically meaningful transcriptional units. Data from multiple DC subsets were analyzed to define coordinately expressed transcripts that were grouped together to define a module. Specifically, the degree of "closeness" between all pairs of genes was defined by Pearson's correlation coefficients. Modules were then compared between species. Strong correlations thus identified genes that have the most similar expression patterns across the samples in the dataset.

Construction of mouse DC transcriptional modules

We took advantage of the large compendium of murine DC expression data that are available through the Immgen database. Overall, we used the WGCNA algorithm on 116 samples encompassing 36 DC subpopulations (Langfelder and Horvath, 2008) to construct and define modules. For each module, representative eigen genes could be defined that reflect the collective behavior of each module. Using this approach, we were able to define each cell type by the behavior of 16 independent modules (Fig. 2 A and Table S1). Each module represented specific components from 19 different pathways (Fig. 2 B). Modules showed a large degree of cell specificity in their expression patterns (Fig. 2 A). For example, expression of module Mm2 was enriched in the lymph node migratory populations of DCs, expression of module

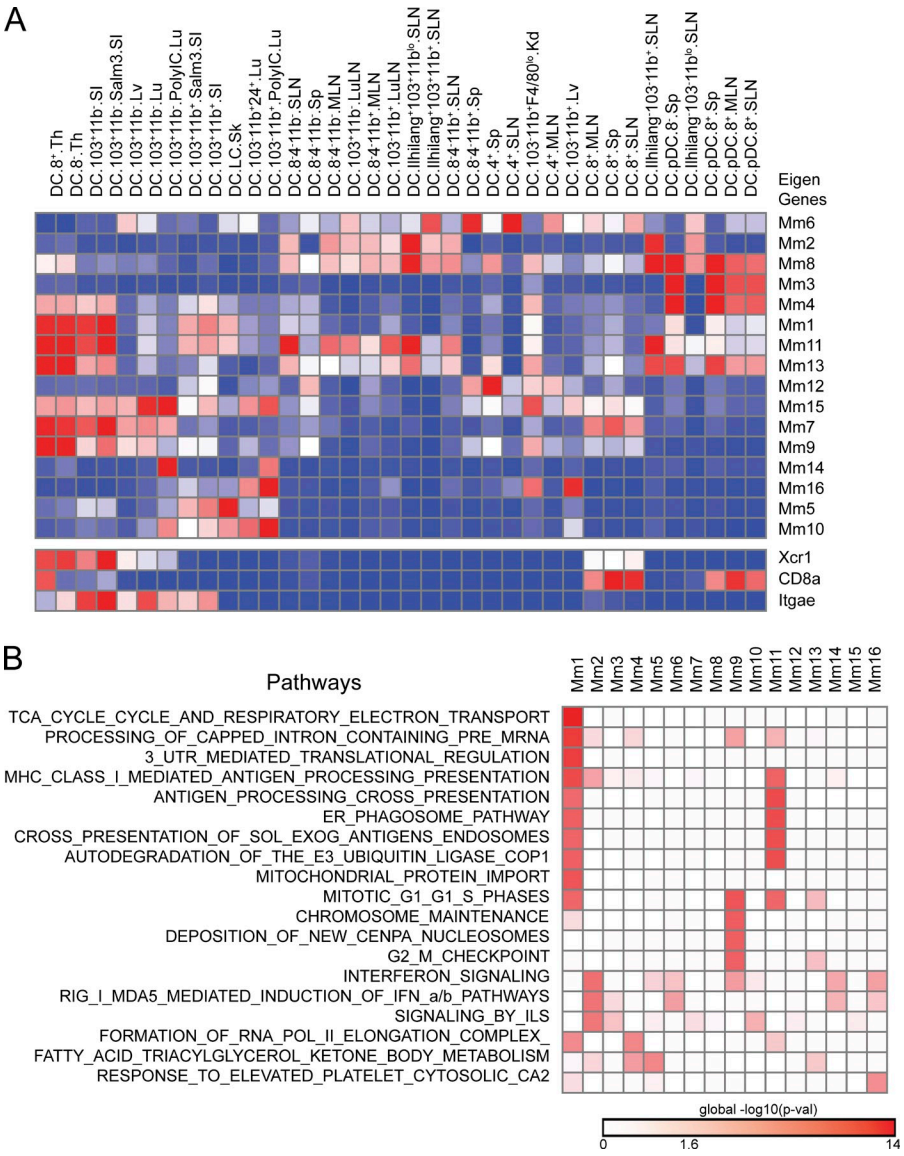

Figure 2. Gene co-expression network analysis identifies conserved transcriptional modules in mouse and human skin DCs. (A) Transcriptional landscape of mouse DCs described in 16 modules (Mm1–Mm16). Expression values for eigen genes corresponding to each module are shown, as well as the expression of xcr1, cd8a, and (Itgae) CD103 as identifiers of cross-presenting subsets (bottom). (B) Enrichment of annotated pathways in individual murine transcriptional modules. Top 19 enriched pathways are shown.

Mm3 was enriched in pDCs, and expression of Mm1 was specific to thymic and $CD103^+CD11b^-$ small intestine subpopulations, whereas expression of Mm6 consisted of genes whose regulation was shared between the $CD4^+$ DCs and $CD103^-CD11b^+$ skin draining lymph node. Along the same lines, module Mm16 included genes specific for $CD103^-CD11b^+$ DCs. Overall the pattern of all 16 subsets was distinct for each cell type.

We characterized each module functionally by comparing components of the module against a database of annotated canonical pathways (Reactome; Matthews et al., 2009). A functional relationship between multiple components was clearly observed in several modules (Fig. 2 B). For instance, module Mm4 is enriched in genes involved in fatty acid metabolism, which is a distinct feature of murine pDCs. In contrast, TCA cycle genes are enriched in Mm1, which is characteristic of thymic DCs. Importantly, Mm1 also showed significant enrichment in genes involved in antigen cross-presentation and related pathways (Fig. 2 B). This module was expressed in thymic and small intestine $CD103^+CD11b^-$ DCs, suggesting that these cell types are particularly efficient in cross-presentation among murine DCs. Importantly, expression of XCR1, the definitive marker of cross-presenting cell types in mice (Bachem et al., 2010; Crozat et al., 2010a), was also strongest in these cell types (Fig. 2 A, bottom). Furthermore, these cell types, uniquely expressed CD8α and CD103 (Fig. 2 A, bottom). Thus, transcriptional modules can be used to generate coherent transcriptional and functional units representing distinct subpopulations.

Construction of human skin DC transcriptional modules

To investigate the functional relationship between human DC systems, we analyzed human skin DCs (17 samples spanning four major skin DC subsets) in a manner similar to the approach

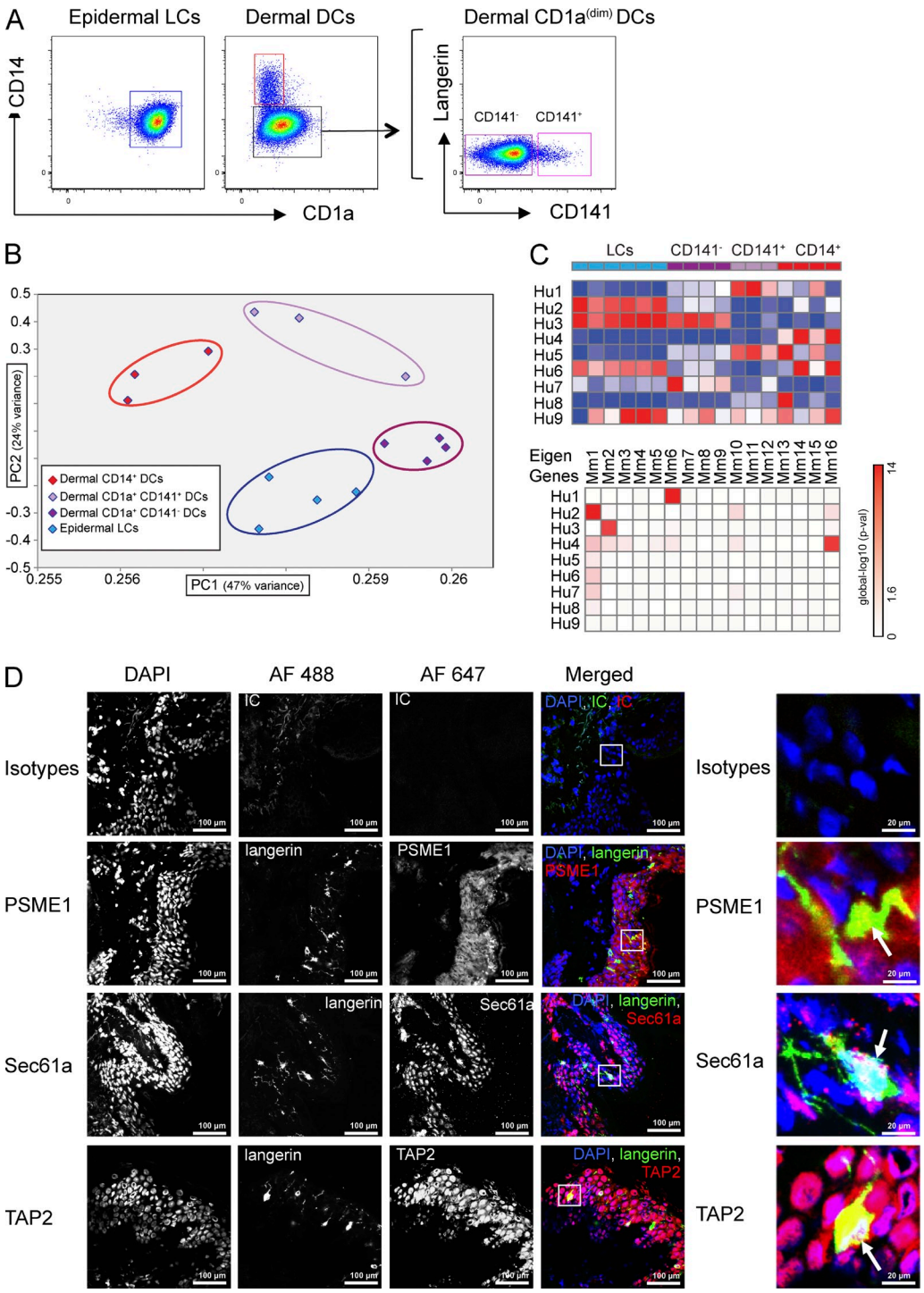

Figure 3. Characterization of human epidermal and dermal DCs. (A) Epidermal- and dermal-resident DCs were allowed to migrate from their respective tissues and were harvested after 2 d. The cells were stained with CD1a and CD14 mAbs, and analyzed by flow cytometry. Epidermal sheets yielded CD1a^{hi}CD14^{-} cells (LCs; blue). Dermis yielded two distinct populations: CD1a^{-}CD14^{+} cells (dermal CD14^{+} DCs; Red) and CD1a$^{(dim)}$CD14^{-} cells (dermal CD1a$^{(dim)}$ DCs). Dermal CD1a$^{(dim)}$Langerin$^{(neg)}$ DC population was further divided into two major sub populations based on CD141 expression (dark and light purple). 1 representative out of at least 30 donors analyzed. (B) Principal component analysis (PCA) of microarray data describing the relationship between the distinct human skin DC subsets: LCs, dermal CD1a$^{(dim)}$CD141^{-}, dermal CD1a$^{(dim)}$CD141^{+}, and dermal CD14^{+} DCs. Plot shows the first two principal components. Data of 3–4 donors from each DC subset are graphed. (C, top) Expression values for nine eigen genes describing transcriptional modules that were identified for four human skin DC subset through Gene Coexpression Network Analysis. (C, bottom) Conservation analysis (through Fisher's exact test) between human and mouse transcriptional modules is shown. Higher red color intensity signified a greater significant overlap between the modules. (D) PSME1, Sec61a, and TAP2 expression in Langerhans cells: 5-µm skin sections were co-stained for nuclei using DAPI (blue), Langerin (AF488

Table 1. The number of genes that are shared between each human and mouse transcriptional module.

Genes	Mouse	701	531	248	157	168	42	98	78	75	92	84	51	49	45	59	40
Human	Module	1	2	3	4	5	6	7	8	9	10	11	12	13	14	15	16
312	1	72	60	37	**23**	16	23	16	16	13	7	3	5	4	7	7	3
794	2	**311**	142	62	53	49	8	25	19	19	15	32	11	20	6	17	5
494	3	124	**157**	34	25	28	3	18	19	18	20	17	9	7	8	6	1
408	4	75	63	61	27	39	1	19	4	13	25	11	12	5	12	16	**25**
90	5	13	14	17	5	8	2	6	2	0	6	2	4	1	1	6	3
192	6	75	40	13	9	9	2	5	5	6	1	10	5	5	3	3	1
139	7	17	41	10	10	10	0	6	10	6	12	3	4	4	4	2	0
55	8	6	8	8	5	7	2	1	2	0	5	2	1	1	4	1	2
34	9	8	6	6	0	2	1	2	1	0	1	4	0	2	0	1	0

Bold indicates the the highly similar modules between the human and the mouse DC subsets. Corresponds to Fig. 3 C (bottom).

we used for the mouse data. Our goal was to identify modules of coordinately expressed human DC transcripts and compare them to the modules that we identified in mouse.

As we have previously reported, epidermal sheets yielded $CD1a^{hi}CD14^{-}$HLA-DR^{+} cells expressing Langerin (CD207), a marker of LCs (Fig. 3 A; Klechevsky et al., 2008). Dermal sheets yielded two major populations: HLA-$DR^{+}CD1a^{-}CD14^{+}$ cells (dermal $CD14^{+}$ DCs) and HLA-DR^{+}Langerin$^{(neg)}CD1a^{(dim)}CD14^{-}$ cells (dermal $CD1a^{(dim)}$ DCs; Fig. 3 A and Fig. S1 A, population IV). The latter can be further subdivided into 2 populations based on CD141 expression (Fig. 3 A, right). Studies performed with 32 skin samples revealed that LCs represented ∼36% of all the DCs that were isolated. Dermal $CD1a^{(dim)}$ DCs represented 54% of the viable lineage-negative migrating $FSC^{hi}SSC^{hi}$HLA-DR^{+} cells of which 3% expressed CD141. Dermal $CD14^{+}$ DCs, the second major dermal DC population represented 10% of the migrating $FSC^{hi}SSC^{hi}$HLA-DR^{+} cells (Fig. S1 B).

RNA was purified and expression analysis was performed using microarrays. Principal Component Analysis (PCA), a clustering approach widely used for population stratification, showed a clear separation between individual DC subtypes (Fig. 3 B). Gene co-expression analysis was used to identify the major transcriptional modules expressed in the different human skin DC populations. Nine major modules were identified (Hu1-Hu9; Fig. 3 C, top; and Table S2). Although the expression of a single module could define an individual cell type, we also identified two modules (i.e., Hu3 and Hu6) that were shared between two human skin DC populations. Module Hu3 was shared between LCs and dermal $CD1a^{(dim)}CD141^{-}$ DCs, whereas Hu6 was shared between LCs and dermal $CD14^{+}$ DCs. Thus, human skin DC subsets could be characterized based on transcriptional modules formed by coordinate gene expression.

Using modules to map transcriptional correlates between human dermal DCs and mouse DCs

To determine whether modules overlap between human skin and murine DC subsets, we used Fisher's exact test to measure the similarity between two modules. We found that the composition of several modules were highly similar between murine and human DC systems (Fig. 3 C, bottom; and Table 1).

We then assessed the functional relationship between mouse DCs and individual human skin DC subsets by comparing similarities in expression modules. We found that the module expressed in human dermal $CD14^{+}$ DCs (Hu4) was most similar to the module expressed in murine $CD103^{-}CD11b^{+}$ cells (Mm16; Fig. 3 C). A closer examination showed that these cells also shared an enrichment in genes involved in interferon signaling (RIGI and the MDA5), as well as genes involved in the response to cytosolic Ca^{2+}.

The module expressed in human dermal $CD141^{+}$ skin DCs (Hu1) was conserved with mouse module Mm6. Although mouse Mm6 did not correspond to any single mouse DC subtype, it included genes that were enriched in the mouse $Lang^{high}CD103^{-}CD11b^{+}$ DCs and the $CD4^{+}$ DCs from skin draining lymph nodes (Fig. 2 A). Both mouse $CD11b^{+}$ and $CD4^{+}$ DCs are of similar origin and are BATF3 independent (Hildner et al., 2008). We found that they share common features with the human dermal $CD141^{+}$ DCs (Fig. 3 C). Thus, human dermal $CD141^{+}$ DCs and $CD14^{+}$ DCs corresponded to the mouse $CD4^{+}$ and $CD11b^{+}$ DCs, respectively.

Using modules to map transcriptional analogies between epidermal LCs and mouse DCs

Next, we assessed the relationship between human LCs and mouse DCs using a similar approach. We found that the

channel, green), and either PSME1, Sec61a, or TAP2 (AF647 channel, red) as stated in the Materials and methods section. (left) Staining was observed in three channels corresponding to DAPI, AF488, or AF647 and co-localization between AF488 and AF647 channels was observed in the merged picture. Pictures show one representative z position. DCs expressing PSME1, Sec61a, or TAP2, (co-localization between AF488 and AF647 channel) are highlighted in white squares. (right) 9× numerical zoom on highlighted DCs is shown and white arrows show co-localization between Langerin and markers of interest. Bar, 100 µm. Representative images out of six independent experiments done with four different donors.

Table 2. Canonical pathway enrichment of shared genes

Gene set name	No. genes in gene set (K)	No. genes in overlap (k)	k/K	P-value
TCA cycle and respiratory electron transport	141	28	0.1986	6.66×10^{-33}
VIF mediated degradation of apobec3g	52	16	0.3077	1.04×10^{-22}
Class I MHC mediated antigen processing presentation	251	25	0.0996	9.39×10^{-22}
Antigen processing ubiquitination proteasome degradation	212	23	0.1085	5.87×10^{-21}
Proteasome	48	14	0.2917	1.18×10^{-19}
ER phagosome pathway	61	14	0.2295	5.09×10^{-18}
Cell cycle mitotic	325	24	0.0738	6.79×10^{-18}
Cell cycle	421	26	0.0618	2.22×10^{-17}
Antigen processing cross presentation	76	14	0.1842	1.42×10^{-16}
Cross presentation of soluble exogenous antigens endosomes	48	12	0.25	4.02×10^{-16}
Metabolism of mRNA	284	20	0.0704	1.00×10^{-14}
Regulation of_mRNA stability by proteins that bind au rich elements	84	13	0.1548	1.90×10^{-14}

Enrichment (evaluated by hypergeometric test) of annotated canonical pathways among the genes that are shared between mouse module (Mm)1 and Human module (Hu)2 and which are enriched in the mouse CD8α⁺CD103⁺ cross-presenting DCs and human LCs, respectively. The list of these annotated genes (311) is provided in Table S3 and the pathways are annotated by REACTOME.

human LC-specific module, Hu2 was most similar to the murine cluster, Mm1, a module that was most highly enriched in thymic DCs and in the CD103⁺CD11b⁻ small intestine DCs (Fig. 2 A and 3 C). As shown in Table 1, 311 genes were shared between the human and mouse modules Hu2 and Mm1 and are expressed in the cross-presenting DC subsets in both species: in the mouse CD8α⁺CD103⁺ DCs and in human LCs. Using the hypergeometric test and the MSigDB database, we found that this cross-species signature (provided in Table S3) was significantly enriched for pathways of antigen processing and cross presentation, as well as in related pathways including the ER phagosome pathway (Table 2 and Tables S4 and S5). Genes such as PSME1, SEC61a, and TAP2 that are functionally related to the cross-presentation pathways, as we confirmed by tissue staining, were highly expressed in LCs before their migration out of the skin (Fig. 3 D). In addition, pathways related to tricarboxylic acid (TCA) cycle, metabolism, cell cycle, and mRNA regulation, as well as components of the cross-presentation machinery, i.e., the ER phagosome pathway, were shared (Table 2). Thus, the cross-presenting cell types in mice and humans share common metabolic, cell cycle, and regulatory genes in addition to actual antigen processing and presentation machinery.

Interestingly module Hu3 that corresponded to the mouse module Mm2 contained interferon-related genes and was also shared between human LCs and the CD141⁻ population. Importantly, we did not detect any overlap of modules between mouse and human LCs, suggesting that they are functionally dissimilar. Compared with other DC subtypes in the skin, human LCs were mostly enriched in expressed genes that are annotated as involved in cross-presentation and the expression of this set of genes was most similar to mouse CD8⁺ thymic DCs. This suggested that these two cell types share a similar role in initiating primary responses.

Human LCs express markers of the mouse CD8α⁺/CD103⁺ DCs

To confirm our transcriptomic analysis showing potential function overlap between human LCs and mouse CD8α⁺/CD103⁺ DCs, we assessed using flow cytometry, the expression of several surface receptors that are specifically expressed on the latter. Indeed, CD24, a marker expressed on mouse dermal Langerin⁺CD103⁺ DCs, was also detected on human LCs, but not on any other skin DC subset. Sirpα, a marker that is expressed on mouse macrophages, CD8⁻CD11b⁺ DCs, and mouse LCs, was detected on the dermal CD14⁺ DCs, but not on human LCs (Fig. 4 A). Moreover, human LCs expressed high amounts of BTLA (Fig. 4 A), a marker that is selectively expressed by mouse CD8α⁺ DCs and their tissue counterparts, CD103⁺CD11b⁻ DCs (Han et al., 2004b). Dermal CD1a$^{(dim)}$CD141⁻ DCs also expressed moderate amounts of BTLA in comparison to dermal CD1a$^{(dim)}$CD141⁺ DCs and dermal CD14⁺ DCs that expressed low to undetectable levels of BTLA (Fig. 4 A). Whereas mouse LCs express CD11b, human dermal CD1a$^{(dim)}$ DCs and dermal CD14⁺ DCs, but not human LCs, expressed high-to-intermediate levels of CD11b (Fig. 4 A). All skin DC populations expressed CD11c; however, the epidermal LCs expressed lower levels compared with the dermal subsets (Fig. 4 A). Overall, consistent with our predictions based on our modular analysis, human LCs displayed a greater similarity to the mouse CD11b⁻CD8α⁺/CD103⁺ DCs than to mouse LCs, whereas dermal CD1a$^{(dim)}$CD141⁺ and dermal CD14⁺ DCs displayed similar markers as the mouse CD11b⁺CD8α⁻/CD103⁻ DC subsets.

Human LCs are enriched with genes associated with cross-presentation and migratory capacity

To further confirm our analysis suggesting that LCs function in cross-presentation, we compared the gene expression profile

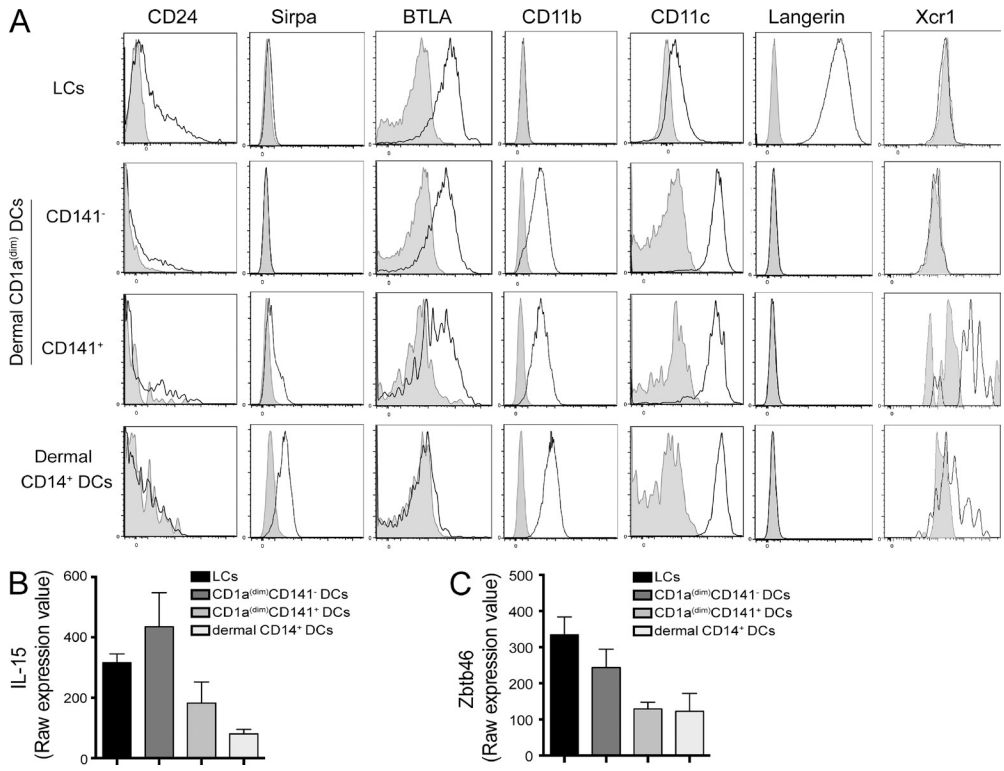

Figure 4. Characterization of human epidermal and dermal DCs. (A) Flow cytometry analysis of isolated epidermal and dermal cells. Cells were gated on epidermal CD1a^{hi} LCs, dermal CD1a$^{(dim)}$ or dermal CD14$^+$ populations and analyzed for the expression of CD11b, CD11c, Langerin, CD24, Sirpα, and BTLA. CD1a^{hi}Langerin$^+$ DCs that were found in the dermal suspension were excluded from this analysis. Representative phenotype of one out of five examined donors. (B and C) Gene expression analysis showing relative amounts of mRNAs expression of IL-15 (A) and Zbtb46 (B) by sorted skin DC subsets: epidermal LCs, dermal CD1a$^{(dim)}$CD141$^-$ DCs, CD1a$^{(dim)}$CD141$^+$ DCs, and CD14$^+$ DCs isolated from at least three different specimens. Mean values ± SEM; $n > 3$ are plotted.

of human LCs to the well-established, cross-presenting human DC subset, blood CD141$^+$ DCs. These cells have been previously shown to be equivalent to the mouse XCR1$^+$CD8α$^+$ DC (Bachem et al., 2010; Crozat et al., 2010a; Jongbloed et al., 2010; Poulin et al., 2010). Using a recently published dataset where various blood DC subsets and monocytes were profiled, we identified a cluster of more than 200 transcripts that were differentially expressed between CD141$^+$ DCs and all other blood DC subtypes (Haniffa et al., 2012; Fig. S2). Gene set enrichment analysis (GSEA; Subramanian et al., 2005) was used to compute the similarity of each DC subset to blood CD141$^+$ DCs relative to the other skin subpopulations. GSEA is used to provide a statistical evaluation for the enrichment of a defined set of genes within a transcriptional profile. The gene set specific to the cross-presenting blood CD141$^+$ DCs was analyzed against the transcriptional profiles of all the different skin DC subsets. Notably, LCs were the only human DC subsets that scored highly for the blood CD141$^+$ DC-derived signature (Fig. 5 A; $P < 10^{-3}$). This confirmed the similarity of LCs with an established cross-presenting DC subset. We performed a complementary analysis by using the set of 200 of the LC-specific genes (Fig. S3 A) that were highly enriched in module Hu2 and then evaluated their enrichment within the blood CD141$^+$ DC dataset. As shown in Fig. 5 B, the human LC-specific signature was enriched in the blood CD141$^+$ DCs.

Next, in an unbiased approach, we performed an analysis to identify the enrichment of previously annotated gene sets in skin DCs. GSEA analysis (Subramanian et al., 2005) confirmed that LCs were significantly enriched ($P < 10^{-3}$) in canonical pathways of antigen processing and cross-presentation (Fig. 5 C), as well as eight other pathways that function as part of the cross-presentation machinery compared with other skin DC subsets, (Fig. S3 B). Finally, the LC-specific signature (Fig. S3 A) was enriched in a gene set that was previously shown to define a migratory DC phenotype in the mouse (Miller et al., 2012; Fig. 5 D). This further supports the DC origin of LCs and distinguishes them from macrophages in tissues. Thus, human LCs are enriched in pathways related to cross-presentation and migration compared with other examined human skin DCs.

LCs are superior at priming naive allogeneic CD8$^+$ T Cells over dermal DCs

To test our observation related to the capacity of LCs to mediate class I–associated presentation, we tested the ability of the different human skin DC subsets to activate allogeneic naive CD8$^+$ T cells (CCR7$^+$CD45RA$^+$CD45RO$^-$). As

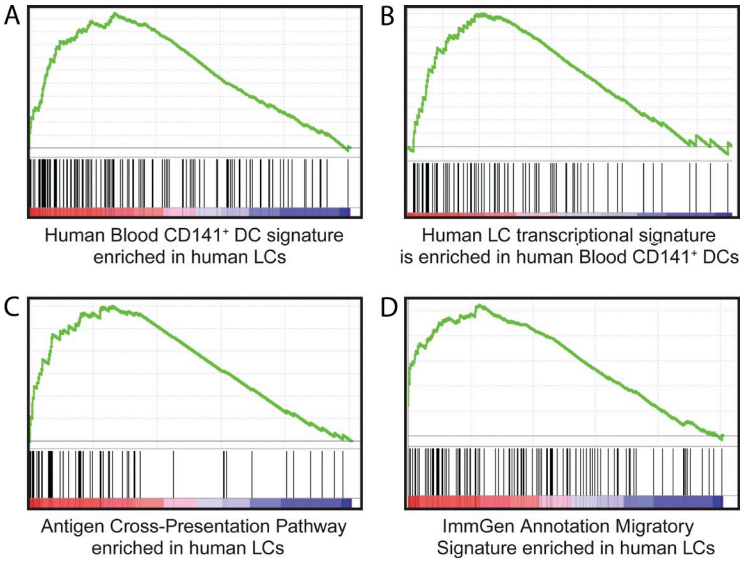

Figure 5. Enrichment of human LC-specific genes in different signatures as computed through GSEA. The GSEA algorithm for the enrichment of a specific gene signature in a gene expression dataset was performed. The genes are first arranged by expression level with the highest expressed genes on the left and the lowest expressed genes on the right. The positions of each of the genes in the "set" or "signature" is depicted by the black lines. The score is a running sum calculated by the expression level of each gene in the signature moving from left to right. (A) Human blood CD141+ DC specific signature among LC genes ($P < 10^{-4}$). Human blood CD141+ DC specific signature was identified as top 200 genes specific for CD141+ DCs relative to other blood DC subtypes based on data from Haniffa et al., 2012 (Fig. S2). (B) LC-specific gene signature (200 most LC-specific genes from module 2, which is enriched in cross-presentation pathway) is enriched in human blood CD141+ DCs ($P < 10^{-4}$). (C) Genes from annotated antigen cross-presentation pathway (REACTOME; $P < 10^{-4}$) and eight other annotated cross-presentation related pathways are also enriched in human LCs (Fig. S3 B). (D) Migratory DC signature defined by Immgen (Miller et al., 2012) in human LCs ($P < 10^{-4}$).

previously reported (Klechevsky et al., 2008; Banchereau et al., 2012b), LCs are powerful stimulators of naive CD8+ T cell proliferation, whereas dermal CD14+ DCs are weak in comparison. Dermal CD1a(dim)CD141− DCs were more efficient at priming allogeneic naive CD8+ T cells compared with the dermal CD1a(dim)CD141+ or to the dermal CD14+ DCs (Fig. 6, A and B). The response was dependent on the number of DCs present in the culture (Fig. 6 C). Activation of the Langerin+ DCs with TLR7/8 or TLR3-agonists did not result in a significant increase in CD8+ T cell proliferation (Fig. 6 D). Dermal CD14+ DCs barely induced any CD8+ T cell proliferation, even after the maturation with TLR3 and TLR7/8 agonist. Within the dermal CD1a(dim) DCs, CD141− DCs induced higher proliferation of naive CD8+ T cells compared with CD141+ cells, particularly upon TLR7/8 activation (Fig. 6 D). In addition, cells cultured over LCs as well as dermal CD1a(dim)CD141− DCs induced allogeneic naive CD8+ T cells to secrete higher amounts of IFN-γ and express activation markers and effector molecules (CD25 and Granzyme B, respectively) compared with the dermal CD1a(dim)CD141+ and dermal CD14+ DCs (Fig. 6 E). Thus, LCs are powerful inducers of naive CD8+ T cell proliferation and differentiation.

LCs efficiently cross-present and cross-prime antigens to CD8+ T cells

Finally, we examined the capacity of each DC subset to cross-present external unprocessed antigens to CD8+ T cells. Human LCs and dermal DC subsets (dermal CD1a(dim)CD141+, CD1a+CD141−, or CD14+ DCs) from an HLA-A201+ donor were loaded with MART-1_{21-35} peptide (YTTAEEAAGIGILTV) that contains the HLA-A201–restricted MART-1 decamer epitope (MART-1_{26-35} EAAGIGILTV) or with the short decamer epitope (MART-1_{26-35} EAAGIGILTV). Cells were then washed and incubated with a CTL clone for 48 h. IFN-γ was measured in the culture supernatant by fluorescent bead array.

All skin DC subsets could present short peptide and induce IFN-γ by the CD8+ T cell clone (Fig. 7 A). However, only LCs and dermal CD1a(dim)CD141− DCs could cross-present the longer peptide to stimulate the CD8+ T cell clone (Fig. 7 B). LCs were more efficient than dermal CD1a(dim)CD141− DCs because as few as 250 cells were sufficient for stimulation (Fig. 7 B, light gray). This is consistent with the increased capacity of LCs to pick up antigen (Fig. 7 C). As expected, both blood myeloid DC subsets (CD1c+ and CD141+ DCs) could present short peptide to the CD8+ T cell clone (Fig. 7 D), but only the CD141+ DCs were able to process long peptide and present it to CD8+ T cells (Fig. 7 E). The ability of blood CD141+ DCs to cross-present required DC activation and was enhanced by TLR3 and TLR7/8 ligation (Fig. 7 E).

To determine the capacity of the DC subsets to cross-present external unprocessed antigens to naive CD8+ T cells, sorted LCs, and dermal DC subsets (dermal CD1a(dim)CD141+, CD1a+CD141−, or CD14+ DCs) were incubated with recombinant MART-1 protein and cultured for 9 d with autologous naive CD8+ T cells and soluble CD40L. CD8+ T cells primed by LCs induced higher amounts of IFN-γ in response to restimulation with MART-1–loaded DCs compared with CD8+ T cells primed by other skin DC subsets (Fig. 7 F). To measure the expansion of epitope-specific T cells, DCs from an HLA-A201+ donor were exposed to MART-1_{21-35} peptide (YTTAEEAAGIGILTV) that contains the HLA-A201–restricted MART-1 decamer epitope (MART-1_{26-35} EAAGIGILTV). Cells were cultured for 10 d with autologous CD8+ T cells purified from the donor skin (Fig. 7 G, top) or from the patient's peripheral blood (Fig. 7 G, bottom). CD40L was added to activate the DCs. As measured using a specific MHC-tetramer, LCs were the most effective at inducing the expansion of MART-1_{26-35}–specific CD8+ T cells compared with the other skin DC subsets (Fig. 7 G). Thus, LCs are highly adept for cross-priming of soluble antigens to CD8+ T cells.

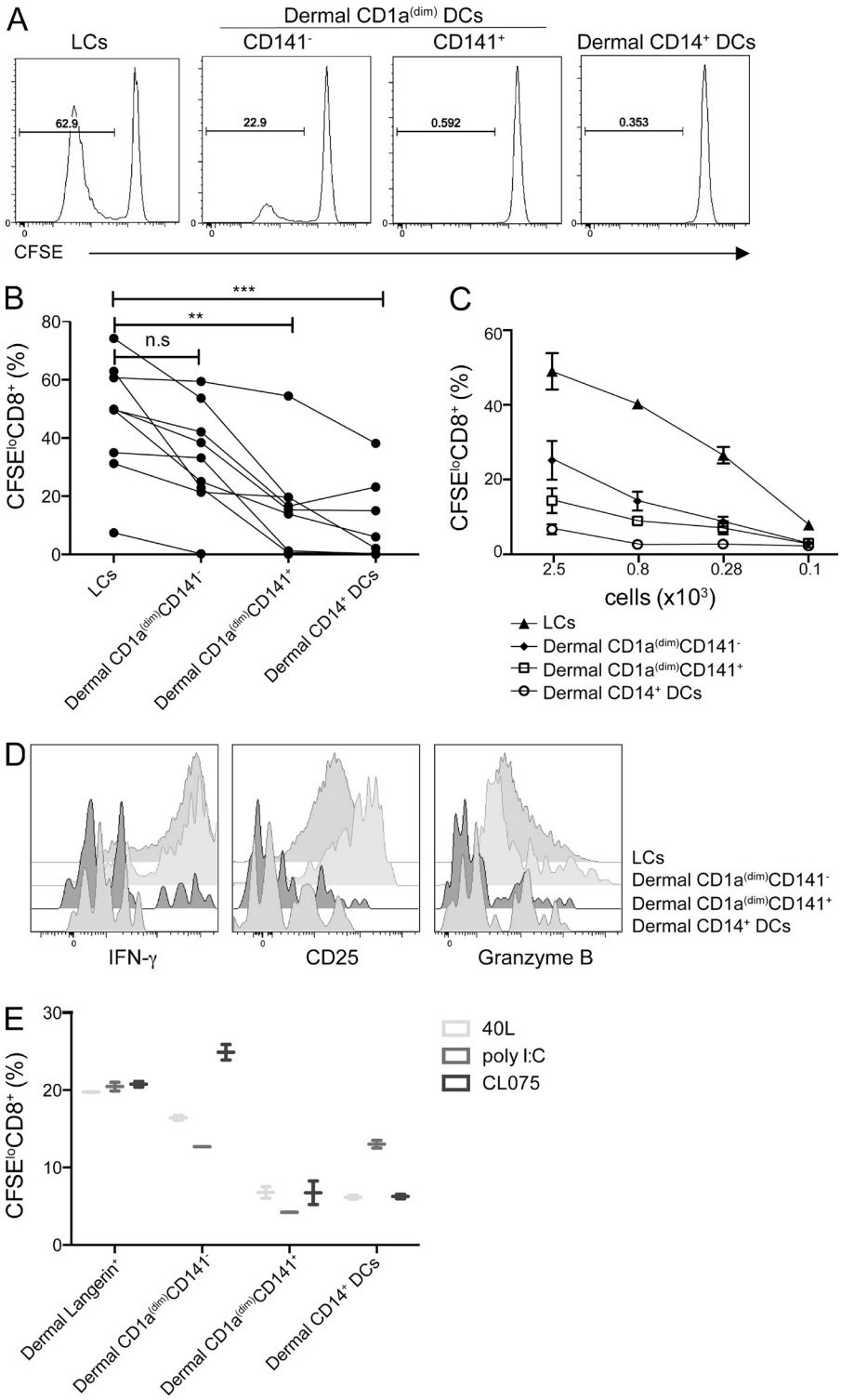

Figure 6. LCs are more efficient than dermal DCs at priming allogeneic naive CD8+ T cells. (A) Proliferation of allogeneic naive CD8+ T cells primed with sorted skin LCs, dermal CD1a(dim)CD141− DCs, dermal CD1a(dim)CD141+ DCs, or dermal CD14+ DCs was measured after 6 d by the dilution of CFSE dye as analyzed by flow cytometry. Histograms show the percentage of proliferating (CFSElo) CD3+CD8+ T cells. Data are representative of eight independent experiments. (B) Graph shows the percentage of proliferating (CFSElo) CD3+CD8+ T cells in nine experiments. (C) Graph shows the percentage of naive CD8+ T cell that diluted CFSE in response to descending numbers of each DC subset that are present in the culture. Graph shows Mean ± SEM; $n = 3$. (D) Graph shows the percentage of naive CD8+ T cell that diluted CFSE in response to each DC subset that were activated with either CD40L, TLR3-agonist (Poly I:C), or TLR7/8-agonist (CLO75). Data are representative of three independent experiments. (E) Allogeneic CFSE-labeled naive CD8+ T cells were primed for 7 d by each skin mDC subset. The proliferating CFSElo cells were stained and analyzed by flow cytometry for the expression of the effector molecules IFN-γ and Granzyme B, as well as the activation marker CD25 upon restimualtion with PMA and Ionomycin. Data are representative of three independent experiments.

DISCUSSION

Characterization of functionally distinct DC subsets in mice acquires special significance if analogous counterparts exist in humans. Unlike the lymphoid system of T and B cells, identifying equivalent DC subsets based on the expression of selected surface receptors has proven to be inaccurate (Crozat et al., 2010b). In this study, we constructed a functional module strategy that takes into account the biological variability inherent to a specific DC subset (Fig. 1). Human systems immunology approaches have already been very powerful to study regulatory networks that underline immune processes (Amit et al., 2011; Buonaguro and Pulendran, 2011). Several

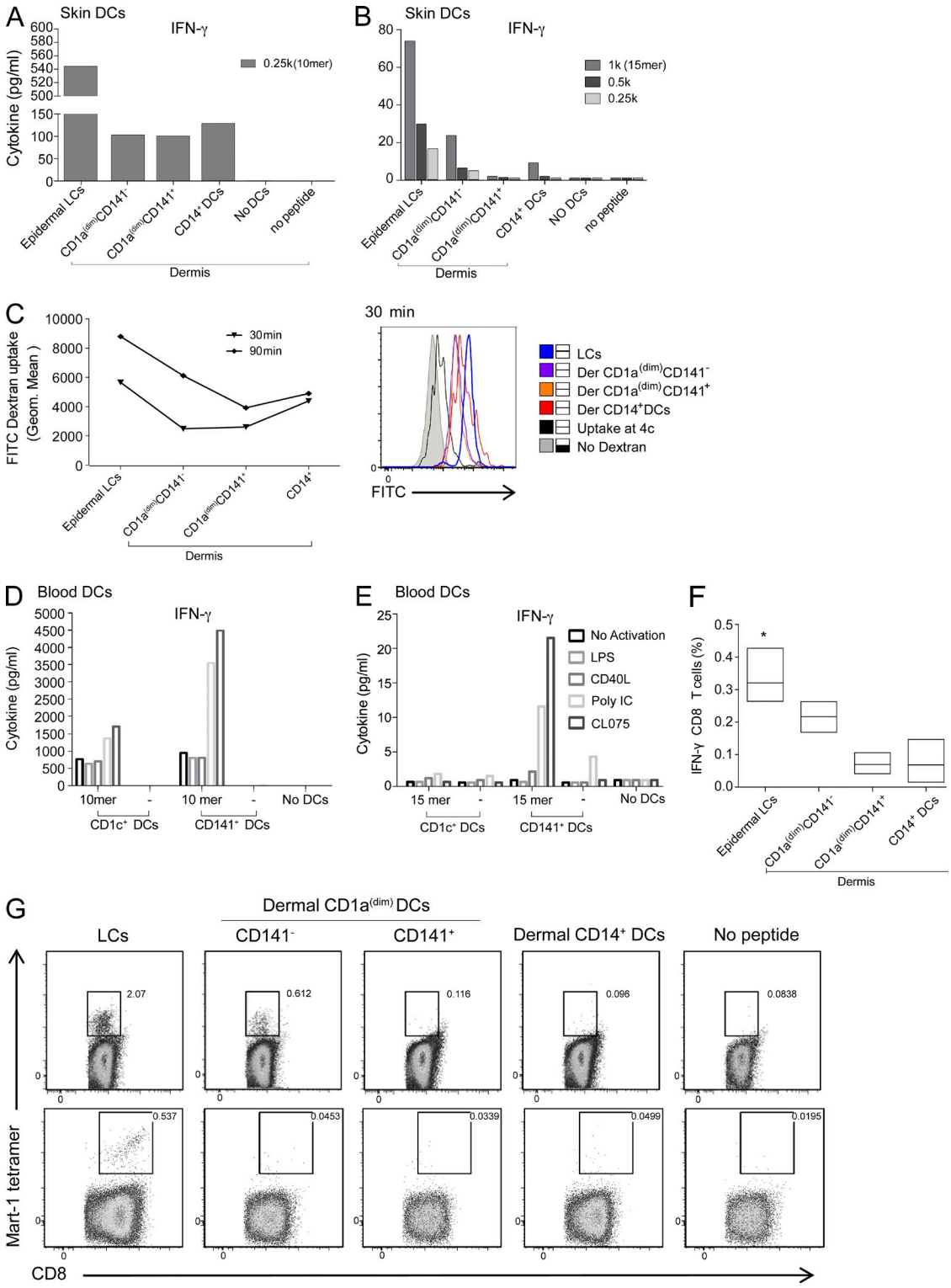

Figure 7. LCs Are highly efficient at cross-presenting and cross-priming antigens to CD8⁺ T cells. (A) Skin DC subsets (LCs, dermal CD1a$^{(dim)}$CD141^{-}, CD1a$^{(dim)}$CD141^{+}, and dermal CD14$^{(dim)}$ DCs) from an HLA-A201^{+} donor were loaded with 10 aa HLA-A201-MART-1–restricted epitope and cultured with a specific CD8^{+} T cell clone. Graph shows the amounts of IFN-γ that were measured in the culture supernatant after 48 h by Luminex. One representative experiment out of three performed. (B) Skin DC subsets (LCs, dermal CD1a$^{(dim)}$CD141^{-}, CD1a^{+}CD141^{+}, and dermal CD14^{+} DCs) from an HLA-A201^{+} donor were loaded with 15 aa MART-1 peptide containing the HLA-A201–restricted epitope and cultured with MART-1–specific CD8^{+} T cell clone. Graph shows the amounts of IFN-γ that were measured in the culture supernatant after 48 h. One representative experiment out of three performed. (C) LCs display more antigen uptake compared with other skin DC subsets. Epidermal or dermal DCs were cultured with 40 kD FITC-labeled Dextran

major advantages of transcriptional co-expression networks make such studies a future step in the genomic understanding of the relationship between mouse and human DCs. First, transcriptional network analysis is less dependent on the magnitude of change in expression of any individual gene. Network analysis elucidates connections between genes and pathways to be revealed that might otherwise have been unappreciated (Han et al., 2004a). Second, network analysis reveals genes and pathways that are predicted to be central to the biological system being analyzed (Jeong et al., 2001). Finally, network analysis identifies modules of highly correlated genes representing transcriptional developmental programs that can serve as comparative factors in determining human mouse analogues. Transcriptional co-expression networks may thus facilitate a deeper understanding of complex cellular systems.

Using this method, we found that human skin DCs share key transcriptional modules with mouse DCs. Specifically, the human dermal $CD14^+$ DCs displayed functional similarities with the mouse $CD103^-CD11b^+$ DCs that was related to MDA and RIGI type I IFN induction and signaling, suggesting that dermal $CD14^+$ DCs might be an important initial source of type I IFN production in response to a viral invasion on the skin, even before the migration of plasmacytoid DCs (pDCs) to the skin.

We also found that human LCs displayed functional similarities with the mouse $CD8\alpha^+$ DC subsets that co-expressed CD103 and the chemokine receptor XCR1. These cells include the mouse thymic and small intestine DCs. Interestingly, both mouse thymic DCs and a unique $CD8\alpha^+CD103^+$ small-intestine DCs were particularly efficient at priming T cell responses (Dresch et al., 2011; Fujimoto et al., 2011). Functionally, human LCs were the most adept at priming allogeneic naive $CD8^+$ T cells into effector CTLs compared with the other skin populations. They were also highly effective at cross-priming soluble antigens to syngeneic naive $CD8^+$ T cells.

LCs have long been considered to be the major sensitizing cells in the skin by initiating protective immunity in naive resting T cells. A role in allergic hypersensitivity was first reported in humans and guinea pigs (Silberberg et al., 1976). They were shown to effectively expand pathogen-specific effector $CD8^+$ T cells, rather than T regulatory (T reg) cells in the skin upon activation (Seneschal et al., 2012). Although in the human these DCs play a critical role in immunity, the relevance of LCs to $CD8^+$ T cell–mediated immunity in mice is still disputed. In particular, mouse LCs were shown to be dispensable over the dermal $Langerin^+CD103^+$ DCs for inducing $CD8^+$ T cell responses in several viral infection, tumor, and self-antigen models (Igyártó et al., 2011; Kautz-Neu et al., 2011; Gomez de Agüero et al., 2012), whereas in other cases they were found to be essential for protective immunity (Sparber et al., 2010; Liard et al., 2012; Wang et al., 2012). The identification of two different types of mouse LCs (Seré et al., 2012) may be important in the interpretation of these studies.

Although this is not the case in mice, the only skin DC subset that expresses Langerin in humans are the Langerhans cells of the epidermis. The best indication is that no Langerin-expressing cells could be detected in the dermis by immunofluorescence staining of human skin tissue (Fig. 3 D). However, occasionally a small proportion (~1%) of $Langerin^+$ cells were found in the dermal cell suspension (Fig. S1 A, gate II). Because these cells expressed higher amounts of CD1a compared with the intermediate dermal CD1a population (Fig. S1 C) and they also expressed EpCam, we surmised that they were likely to represent LCs that migrate through the dermis, as proposed for a similar population that was observed in the mouse (Nagao et al., 2009). Alternatively, they may simply be residues of LCs of the epidermis that remain after its separation from the dermis. Because these cells were too rare to study and we also could not exclude the fact that these might be contaminating LCs, we excluded them from the current analysis.

Previously identified differences between mouse and human LCs may, however, further help explain the discrepancy between the two species. For example, in the mouse, LCs resemble tissue-resident macrophages; they are developmentally dependent on M-CSFR (Ginhoux et al., 2006; Wang et al., 2012), express macrophage-specific markers such as F4/80 and CD11b, migrate poorly to lymph nodes relative to the migration of conventional DCs to lymph nodes, constitutively secrete IL-10 (Igyarto et al., 2009), and

at conc. 1 mg/ml at either 4°C or 37°C. The uptake was measured by the amount of FITC fluorescence in the cells after 30 or 90 min by flow cytometry. Cells that were not exposed to beads served as an additional control. (right) Histograms show FITC uptake by the different DC subsets at 30 min. (left) Graph shows FITC geometric mean as measured for the different skin DC subsets after 30 and 90 min. One representative experiments of three performed. (D) Blood DC subsets ($CD1c^+$ and $CD141^+$) from an $HLA\text{-}A201^+$ donor were loaded with 10 aa HLA-A201-MART-1–restricted epitope and cultured with a specific $CD8^+$ T cell clone. Graph shows the amounts of IFN-γ that were measured in the culture supernatant after 48h by Luminex. One representative experiments out of three performed. (E) Blood DC subsets ($CD1c^+$ and $CD141^+$) from an $HLA\text{-}A201^+$ donor were loaded with 15 aa MART-1 peptide containing the HLA-A201–restricted epitope and cultured with MART-1–specific $CD8^+$ T cell clone. Graph shows the amounts of IFN-γ that were measured in the culture supernatant after 48 h. One representative experiment out of three performed. (F) To assess cross-priming, skin DC subsets were incubated with a MART-1 protein and autologous naive $CD8^+$ T cells. After 9 d, IFN-γ–producing $CD8^+$ T cells were assessed by flow cytometry upon restimulation with fresh MART-1–loaded DCs. (Graph shows mean ± SEM; $n = 3$). (G, top) To assess the cross-priming of a specific MART-1 $CD8^+$ T cell epitope, skin DC subsets (LCs, dermal $CD1a^{(dim)}CD141^-$, $CD1a^{(dim)}CD141^+$, and dermal $CD14^+$ DCs) from an $HLA\text{-}A201^+$ donor were incubated with 15 aa MART-1 peptide containing the HLA-A201–restricted epitope and with autologous purified $CD8^+$ T cells for the donor's skin. After 10 d, the number of MART-1–specific $CD8^+$ T cells was determined by the binding of a specific tetramer. (bottom) Similar to the top, except that $CD8^+$ T cells were purified from the donor's blood. Two representative experiments of six performed.

have little to no expression of Zbtb46. This suggests a macrophage identity rather than a DC identity (Meredith et al., 2012; Satpathy et al., 2012). On the contrary, human LCs do not express any of the macrophage markers, they are negative for CD11b, express IL-15 (Klechevsky et al., 2008; Banchereau et al., 2012a) and Zbtb46 (Fig. S4, B and C). This supports their DC identity, and is consistent with their capacity to prime T cells. Contrary to this, human LCs display similar markers to the mouse CD8α$^+$/CD103$^+$ DCs, including BTLA and CD24. Although human LCs lacked the expression of XCR1 (Fig. 4 A), a marker on a mouse cross-presenting DC subset, they were highly enriched in functional modules shared with the mouse XCR1 populations. This further extenuating the lack of significance in using individual markers as a correlative factors in determining human/mouse analogues. Overall, the expression of XCR1 on dermal CD1a$^{(dim)}$CD141$^+$ DCs and on dermal CD14$^+$, but not on LCs or dermal CD1a$^{(dim)}$CD141$^-$ further suggests that XCR1 may not faithfully mark the cross-presenting DC subset in human.

Although in blood, CD141 marks a small population of cross-presenting DC subset (Jongbloed et al., 2010), in human skin, CD141 is detected on multiple populations, including on a small subset of the dermal CD1a$^{(dim)}$ DCs and on the dermal CD14$^+$ DCs (Chu et al., 2012; Haniffa et al., 2012), but not on LCs. Thus, similar to XCR1, CD141 on its own may not be sufficient to mark a cross-presenting tissue DC subset. Overall, systemic genomic comparison, as we have done for all four human skin DC populations, and ensuing functional comparison is the most reliable approach to determine such homologies.

Our study shows that LCs are enriched in genes related to the cross-presentation pathway. Interestingly, we found that this set of genes is enriched in the blood CD141$^+$ DCs gene transcript, the proposed equivalent to the mouse CD8α$^+$ DCs (Bachem et al., 2010; Crozat et al., 2010a), but not in other examined blood antigen-presenting cells. In a different analysis we showed that blood CD141$^+$ DC-specific signature is enriched in LCs and not other skin DC subsets. This suggests that CD141$^+$ DCs, LCs and the CD8α$^+$ DCs share a common transcriptional signature associated with cross-presentation. Although human blood CD141$^+$ DCs are considered the cross-presenting gold standard and the mouse CD8α$^+$ DC homologue, Cohn et al., recently showed that receptor mediated delivery of antigen could facilitate cross-presentation in blood CD1c$^+$ DCs (Cohn et al., 2013). Because we tested only soluble antigen, we suspect that the cross-presentation signature is required for soluble antigen cross-presentation and not antigen directed into early endosomes. In addition, Segura et al. showed that CD1c$^+$ DCs isolated from tonsils cross-present as efficiently as tonsil CD141$^+$ DCs (Segura et al., 2013). Taken the differences observed between skin CD141$^+$ DCs and blood CD141$^+$ DCs, we suspect that tissue CD141$^+$ DCs are different from blood. Overall, CD141 may also not faithfully mark the cross-presenting DC subset across all organs in human.

In the mouse, early cells of the CD8α$^+$ DC lineage are not initially able to cross-present antigens, rather this capability is induced as a later developmental step via TLR ligation or exposure to GM-CSF. Similarly, it was shown that the capacity of human blood CD141$^+$ DCs to cross-present is dependent on TLR ligands such as poly I:C (Fig. 7 D; Haniffa et al., 2012). In that respect, human blood CD141$^+$ DCs could represent the equivalent of an earlier CD8α lineage DCs in mice, where additional factors are also needed to induce the ability to cross-present antigens. Human blood-originated dermal CD141$^+$CD11c$^-$ cells were reported to require TLR activation for efficient cross-presentation (Haniffa et al., 2012). The ability to cross-prime antigen to naive T cells without a requirement of a TLR activation is thought to be a unique property of thymic DCs (Dresch et al., 2011). Here, we show that LCs display a similar capacity and efficient cross-priming could be demonstrated in the absence of TLR stimulation (Fig. 7). This is consistent with our data showing their transcriptional similarity to thymic DCs. Consistent with that, LCs express a very limited set of TLRs as previously reported (Flacher et al., 2006; Klechevsky et al., 2009).

In summary, our study highlights novel functional similarities between human and mouse DC systems. Most profoundly, between the dermal CD14$^+$ DCs and the mouse CD11b$^+$CD103$^-$ and between human epidermal LCs and the mouse XCR1$^+$CD8α$^+$CD103$^+$ DCs. Surprisingly, although mouse and human LCs share some of their markers and their physical location of the epidermis, they differ in their functional module gene expression, which may in fact be more relevant for experimental modules. Overall, our findings demonstrate that human but not mouse LCs are enriched in cross-presentation–specific models. Thus, providing further insight as to the role of LCs in human as cross-presenters of soluble antigens and efficient activators of CD8$^+$ T cells.

MATERIALS AND METHODS

Isolation of skin DC subsets. Human skin specimens were obtained from donors who underwent cosmetic surgeries at Washington University School of Medicine (St. Louis, MO) and Barnes Jewish Hospital (St. Louis, MO) in accordance with Institutional Review Board guidelines. LCs, CD1a$^{(dim)}$, and CD14$^+$ dermal DCs were purified from normal human skin. Specimens were incubated with the bacterial protease, dispase type 2, for 18 h at 4°C. Epidermal and dermal sheets were separated and placed in RPMI 1640 supplemented with 10% fetal bovine serum. After 2 d, the cells that migrated into the medium were enriched using a Ficoll-diatrizoate gradient. DCs were purified by cell sorting after staining with anti-CD1a FITC and anti-CD14 APC mAbs. CD40L (200 ng/ml; R&D Systems) or TLR3 (poly I:C; 10 μg/ml), TLR4 (LPS; 25 ng/ml), and TLR7/8 (CLO75; 1 μg/ml) agonists were used to activate the cells as indicated.

Microarray data acquisition and processing. RNA from sorted populations was purified using TRIzol. RNA was processed, amplified, labeled, and hybridized at Washington University Core Facility (GTAC) with Illumina HumanHT-12 v4 Expression BeadChip. Data were background subtracted and quantile normalized. Normalized mouse DC Immgen dataset was downloaded from the official website.

Gene co-expression network analysis. To address the functional relationship between DCs in mouse and human we assembled two comprehensive datasets: a murine DC dataset that contains 36 different DC subpopulations (3–4 replicates per subtype) derived from the Immgen Database of mouse immune cells and a human skin DC dataset that spanned 4 major skin-resident DC subpopulations from multiple human donors. For the human skin DC dataset, only genes with an average expression value greater than 150 were kept, amounting to 6134 genes. Modules were identified using weighted gene co-expression network analysis (WGCNA) R package (Langfelder and Horvath, 2008). We used Pearson's correlation coefficient as metrics with a power parameter of 12, determined as the power at which scale-free characteristics of the network reached a plateau. Additional parameters were minModuleSize = 100, reassignThreshold = 0.2, mergeCutHeight = 0.1, maxBlockSize = 10,000, deepSplit = 2. Genes with average expression >150 were kept, amounting to 8,059 genes. For module identification, WGCNA algorithm was used with a power parameter of 10. To compute the statistical significance of overlap between modules we used Fisher's exact test.

The GSEA algorithm was performed as previously described (Subramanian et al., 2005). In brief, to test for the enrichment of a specific gene signature in a gene expression dataset, the genes are first arranged by expression level with the highest expressed genes on the left and the lowest expressed genes on the right. The positions of each of the genes in the "set" or "signature" are depicted by the black lines. The score is a running sum calculated by the expression level of each gene in the signature moving from left to right.

Skin DC analysis by immunofluorescence. Skin specimens were embedded in OCT and frozen. 5-µm sections were cut using the Leica CM 1950. For immunofluorescent staining, tissue sections were fixed in 4% PFA for 10 min at room temperature and washed with PBS containing 3% BSA and 10% saponin. Sections were quenched with 0.5 M Glycine for 5 min, washed, and blocked with PBS/BSA/Sapo for 30 min at room temperature. Tissue sections were incubated overnight at 4°C with either polyclonal rabbit anti–human antibodies, PSME1 (2.5 µg/ml; Novus Biologicals), Sec61a (0.5 µg/ml; Pierce Antibodies), TAP2 (2 µg/ml; LifeSpan BioScience) or an isotype control. All sections were stained for mouse anti–human Langerin (CD207; 2 µg/ml; Beckman Coulter) overnight at 4°C. Sections were then washed and incubated with anti–mouse Alexa Fluor 488 (1/200) and donkey anti–rabbit Alexa Fluor 647 (0.6 µg/ml; Jackson ImmunoResearch Laboratories) for 2 h followed by 4',6'-diamidino-2-phénylindole (DAPI) for 10 min at room temperature. Sections were then washed in PBS and mounted (Invitrogen). Images were acquired using an Olympus Confocal Microscope FV1000 using Fluoview software. Image analysis was performed using ImageJ software.

Statistical analyses. Two-sample Student's *t* test was used to calculate differentially expressed genes. For cell-specific signatures, the top 200 up-regulated genes were taken. Mouse to human orthology mapping was performed with the biomaRt R package (Durinck et al., 2005, 2009). For pathway analysis, we used the GSEA (Subramanian et al., 2005) and MSigDb (Broad Institute).

Antigen uptake. Epidermal or dermal DCs were cultured at 37°C with or without FITC-labeled 40KDa dextran (Nanocs Inc.). After 30 or 90 min, cells were harvested and washed with cold media. They were then stained for DC markers and analyzed by flow cytometry. The intensity of the FITC signal was determined for each DC subset. Cells cultured with FITC-dextran at 4°C served as an additional control.

DC/T cell co-cultures. Naive $CD8^+$ T cells were sorted as $CD45RA^+$ $CCR7^+HLA\text{-}DR^-CD8^+$ cells. Allogeneic primed $CD8^+$ T cells were characterized for the expression of the cytotoxic effector molecules Granzyme B (Molecular Probes) and activation molecule CD25 (BD) after 7 d of co-culture with the different DC subsets. Cell proliferation was determined by the level of cell tracer carboxyfluorescein succinimidyl ester (CFSE) dilution at the end of the culture. IFN-γ production (BD) was assessed by flow cytometry after an additional 5-h stimulation with PMA (25 ng/ml; Sigma-Aldrich) and ionomycin (1 µM; Sigma-Aldrich). For autologous cross-priming responses, $CD8^+$ T cells (1×10^5 cells/well) were stimulated with autologous skin DC subsets (2.5×10^4 cells/well) that were incubated with the MART-1 protein or 15 aa $MART\text{-}1_{21\text{-}35}$ peptide (YTTAEEAAGIGILTV). Cells were cultured for 9 d in with 10 U/ml IL-7 (R&D Systems) and 100 ng/ml CD40L (R&D Systems). IL-2 was added at 10 U/ml at day three. Cross-priming was assessed by the expansion of specific CTLs binding a specific $HLA\text{-}A201^+$ tetramer. For intracellular cytokine analysis, day seven-primed $CD8^+$ T cells were restimulated for six hours with antigen-loaded fresh DCs in fresh medium containing CD40L. Surface CD25 expression and intracellular IFN-γ and Granzyme B (all from BD) were assessed by flow cytometry. Cytokines in the culture supernatant of $CFSE^{lo}CD11c^-CD4^-CD8^+$ T cells (1.5×10^5 cells per ml) were measured using a multiplex bead assay Luminex after 48 h of restimulation with anti-CD3 and anti-CD28 mAbs. For the cross-presentation assay, sorted $HLA\text{-}A201^+$ skin or blood DC subsets were incubated (2,500 cells/well) in U-bottom 96-well plates with 1 µM 15 aa MART-1 peptide (YTTAEEAAGIGILTV) or Mart-1 short peptide (ELAGIGILTV) or without peptide for 3 h in RPMI medium. After extensive washing, DCs were cultured with MelanA–specific $CD8^+$ T cell clone (20,000 cells) in RPMI medium supplemented with 10% human serum. Supernatants were collected and analyzed for IFN-γ concentration by Luminex. DC activation was added as indicated.

Accession no. Microarray dataset is available through Gene Expression Omnibus under accession no. GSE66355.

Online supplemental material. Fig. S1 shows the gating strategy and description of dermal DC populations in the skin. Fig. S2 shows the human blood CD141 DC-specific gene signature as derived compared with the other blood APCs. Fig. S3 shows human LC-specific gene signature as derived compared with the other skin DC subsets and enrichment of various expression signatures in skin epidermal LCs relative to other skin DC subtypes. Table S1, available as an Excel file, lists the genes that comprise each of the 16 mouse modules. Table S2, available as an Excel file, lists the genes that comprise each of the 9 human modules. Table S3, available as an Excel file, shows the cross-presenting gene signature list of 311 genes that are shared between mouse module (Mm)1 and human module (Hu)2. Table S4, available as an Excel file,lists the genes that are shared between the mouse ($CD103^+CD8\alpha^+$) and human (LCs) cross-presenting DC subsets. Table S5, available as an Excel file, lists the REACTOME annotated 76 and 48 genes that belong to the antigen processing and cross-presentation, and the cross-presentation of soluble exogenous antigens endosomes pathways, respectively. Online supplemental material is available at http://www.jem.org/cgi/content/full/jem.20131675/DC1.

We thank Drs. Paul Allen, Marco Colonna, Erica Maria Lantelme, Samuel S.K. Lam, and Catherine Martel, as well as Dorjan Brinja, and Stephanie Rodriguez at Washington University School of Medicine Department of Pathology and Immunology for their help. We thank the surgeons, nurses, and staff at the Barnes Jewish Hospital and Washington University School of Medicine Department of Surgery for providing access to skin samples. We thank Drs. Gwendolyn Randolph, Robert Schreiber, and Andrey Shaw for continuous support and critical reading of the manuscript.

This study was supported partly through a grant from Immuneering corp to M.N. Artyomov and funding from Washington University School of Medicine, Department of Pathology and Immunology to E. Klechevsky.

The authors declare no competing financial interests.

Submitted: 8 August 2013
Accepted: 1 April 2015

REFERENCES

Amit, I., A. Regev, and N. Hacohen. 2011. Strategies to discover regulatory circuits of the mammalian immune system. *Nat. Rev. Immunol.* 11:873–880.

Bachem, A., S. Güttler, E. Hartung, F. Ebstein, M. Schaefer, A. Tannert, A. Salama, K. Movassaghi, C. Opitz, H.W. Mages, et al. 2010. Superior antigen cross-presentation and XCR1 expression define human CD11c+CD141+ cells as homologues of mouse CD8+ dendritic cells. *J. Exp. Med.* 207:1273–1281. http://dx.doi.org/10.1084/jem.20100348

Banchereau, J., and R.M. Steinman. 1998. Dendritic cells and the control of immunity. *Nature.* 392:245–252. http://dx.doi.org/10.1038/32588

Banchereau, J., L. Thompson-Snipes, S. Zurawski, J.P. Blanck, Y. Cao, S. Clayton, J.P. Gorvel, G. Zurawski, and E. Klechevsky. 2012a. The differential production of cytokines by human Langerhans cells and dermal CD14(+) DCs controls CTL priming. *Blood.* 119:5742–5749. http://dx.doi.org/10.1182/blood-2011-08-371245

Banchereau, J., S. Zurawski, L. Thompson-Snipes, J.P. Blanck, S. Clayton, A. Munk, Y. Cao, Z. Wang, S. Khandelwal, J. Hu, et al. 2012b. Immunoglobulin-like transcript receptors on human dermal CD14+ dendritic cells act as a CD8-antagonist to control cytotoxic T cell priming. *Proc. Natl. Acad. Sci. USA.* 109:18885–18890. http://dx.doi.org/10.1073/pnas.1205785109

Berry, M.P., C.M. Graham, F.W. McNab, Z. Xu, S.A. Bloch, T. Oni, K.A. Wilkinson, R. Banchereau, J. Skinner, R.J. Wilkinson, et al. 2010. An interferon-inducible neutrophil-driven blood transcriptional signature in human tuberculosis. *Nature.* 466:973–977. http://dx.doi.org/10.1038/nature09247

Buonaguro, L., and B. Pulendran. 2011. Immunogenomics and systems biology of vaccines. *Immunol. Rev.* 239:197–208. http://dx.doi.org/10.1111/j.1600-065X.2010.00971.x

Chaussabel, D., C. Quinn, J. Shen, P. Patel, C. Glaser, N. Baldwin, D. Stichweh, D. Blankenship, L. Li, I. Munagala, et al. 2008. A modular analysis framework for blood genomics studies: application to systemic lupus erythematosus. *Immunity.* 29:150–164. http://dx.doi.org/10.1016/j.immuni.2008.05.012

Chu, C.C., N. Ali, P. Karagiannis, P. Di Meglio, A. Skowera, L. Napolitano, G. Barinaga, K. Grys, E. Sharif-Paghaleh, S.N. Karagiannis, et al. 2012. Resident CD141 (BDCA3)$^+$ dendritic cells in human skin produce IL-10 and induce regulatory T cells that suppress skin inflammation. *J. Exp. Med.* 209:935–945. http://dx.doi.org/10.1084/jem.20112583

Cohn, L., B. Chatterjee, F. Esselborn, A. Smed-Sörensen, N. Nakamura, C. Chalouni, B.C. Lee, R. Vandlen, T. Keler, P. Lauer, et al. 2013. Antigen delivery to early endosomes eliminates the superiority of human blood BDCA3$^+$ dendritic cells at cross presentation. *J. Exp. Med.* 210:1049–1063. http://dx.doi.org/10.1084/jem.20121251

Crozat, K., R. Guiton, V. Contreras, V. Feuillet, C.A. Dutertre, E. Ventre, T.P. Vu Manh, T. Baranek, A.K. Storset, J. Marvel, et al. 2010a. The XC chemokine receptor 1 is a conserved selective marker of mammalian cells homologous to mouse CD8alpha+ dendritic cells. *J. Exp. Med.* 207:1283–1292. http://dx.doi.org/10.1084/jem.20100223

Crozat, K., R. Guiton, M. Guilliams, S. Henri, T. Baranek, I. Schwartz-Cornil, B. Malissen, and M. Dalod. 2010b. Comparative genomics as a tool to reveal functional equivalences between human and mouse dendritic cell subsets. *Immunol. Rev.* 234:177–198. http://dx.doi.org/10.1111/j.0105-2896.2009.00868.x

Doering, T.A., A. Crawford, J.M. Angelosanto, M.A. Paley, C.G. Ziegler, and E.J.Wherry. 2012. Network analysis reveals centrally connected genes and pathways involved in CD8+ T cell exhaustion versus memory. *Immunity.* 37:1130–1144. http://dx.doi.org/10.1016/j.immuni.2012.08.021

Dresch, C., M. Ackermann, B. Vogt, B. de Andrade Pereira, K. Shortman, and C. Fraefel. 2011. Thymic but not splenic CD8$^+$ DCs can efficiently cross-prime T cells in the absence of licensing factors. *Eur. J. Immunol.* 41:2544–2555. http://dx.doi.org/10.1002/eji.201041374

Durinck, S., Y. Moreau, A. Kasprzyk, S. Davis, B. De Moor, A. Brazma, and W. Huber. 2005. BioMart and Bioconductor: a powerful link between biological databases and microarray data analysis. *Bioinformatics.* 21:3439–3440. http://dx.doi.org/10.1093/bioinformatics/bti525

Durinck, S., P.T. Spellman, E. Birney, and W. Huber. 2009. Mapping identifiers for the integration of genomic datasets with the R/Bioconductor package biomaRt. *Nat. Protoc.* 4:1184–1191. http://dx.doi.org/10.1038/nprot.2009.97

Flacher, V., M. Bouschbacher, E. Verronèse, C. Massacrier, V. Sisirak, O. Berthier-Vergnes, B. de Saint-Vis, C. Caux, C. Dezutter-Dambuyant, S. Lebecque, and J. Valladeau. 2006. Human Langerhans cells express a specific TLR profile and differentially respond to viruses and Gram-positive bacteria. *J. Immunol.* 177:7959–7967. http://dx.doi.org/10.4049/jimmunol.177.11.7959

Fujimoto, K., T. Karuppuchamy, N. Takemura, M. Shimohigoshi, T. Machida, Y. Haseda, T. Aoshi, K.J. Ishii, S. Akira, and S. Uematsu. 2011. A new subset of CD103+CD8alpha+ dendritic cells in the small intestine expresses TLR3, TLR7, and TLR9 and induces Th1 response and CTL activity. *J. Immunol.* 186:6287–6295. http://dx.doi.org/10.4049/jimmunol.1004036

Gautier, E.L., T. Shay, J. Miller, M. Greter, C. Jakubzick, S. Ivanov, J. Helft, A. Chow, K.G. Elpek, S. Gordonov, et al. Immunological Genome Consortium. 2012. Gene-expression profiles and transcriptional regulatory pathways that underlie the identity and diversity of mouse tissue macrophages. *Nat. Immunol.* 13:1118–1128. http://dx.doi.org/10.1038/ni.2419

Ginhoux, F., F. Tacke, V. Angeli, M. Bogunovic, M. Loubeau, X.M. Dai, E.R. Stanley, G.J. Randolph, and M. Merad. 2006. Langerhans cells arise from monocytes in vivo. *Nat. Immunol.* 7:265–273. http://dx.doi.org/10.1038/ni1307

Gomez de Agüero, M., M. Vocanson, F. Hacini-Rachinel, M. Taillardet, T. Sparwasser, A. Kissenpfennig, B. Malissen, D. Kaiserlian, and B. Dubois. 2012. Langerhans cells protect from allergic contact dermatitis in mice by tolerizing CD8(+) T cells and activating Foxp3(+) regulatory T cells. *J. Clin. Invest.* 122:1700–1711. http://dx.doi.org/10.1172/JCI59725

Han, J.D., N. Bertin, T. Hao, D.S. Goldberg, G.F. Berriz, L.V. Zhang, D. Dupuy, A.J. Walhout, M.E. Cusick, F.P. Roth, and M. Vidal. 2004a. Evidence for dynamically organized modularity in the yeast protein-protein interaction network. *Nature.* 430:88–93. http://dx.doi.org/10.1038/nature02555

Han, P., O.D. Goularte, K. Rufner, B. Wilkinson, and J. Kaye. 2004b. An inhibitory Ig superfamily protein expressed by lymphocytes and APCs is also an early marker of thymocyte positive selection. *J. Immunol.* 172:5931–5939. http://dx.doi.org/10.4049/jimmunol.172.10.5931

Haniffa, M., A. Shin, V. Bigley, N. McGovern, P. Teo, P. See, P.S. Wasan, X.N. Wang, F. Malinarich, B. Malleret, et al. 2012. Human tissues contain CD141hi cross-presenting dendritic cells with functional homology to mouse CD103+ nonlymphoid dendritic cells. *Immunity.* 37:60–73. http://dx.doi.org/10.1016/j.immuni.2012.04.012

Hildner, K., B.T. Edelson, W.E. Purtha, M. Diamond, H. Matsushita, M. Kohyama, B. Calderon, B.U. Schraml, E.R. Unanue, M.S. Diamond, et al. 2008. Batf3 deficiency reveals a critical role for CD8alpha+ dendritic cells in cytotoxic T cell immunity. *Science.* 322:1097–1100. http://dx.doi.org/10.1126/science.1164206

Igyarto, B.Z., M.C. Jenison, J.C. Dudda, A. Roers, W. Müller, P.A. Koni, D.J. Campbell, M.J. Shlomchik, and D.H. Kaplan. 2009. Langerhans cells suppress contact hypersensitivity responses via cognate CD4 interaction and langerhans cell-derived IL-10. *J. Immunol.* 183:5085–5093. http://dx.doi.org/10.4049/jimmunol.0901884

Igyártó, B.Z., K. Haley, D. Ortner, A. Bobr, M. Gerami-Nejad, B.T. Edelson, S.M. Zurawski, B. Malissen, G. Zurawski, J. Berman, and D.H. Kaplan. 2011. Skin-resident murine dendritic cell subsets promote distinct and opposing antigen-specific T helper cell responses. *Immunity.* 35:260–272. http://dx.doi.org/10.1016/j.immuni.2011.06.005

Jeong, H., S.P. Mason, A.L. Barabási, and Z.N. Oltvai. 2001. Lethality and centrality in protein networks. *Nature.* 411:41–42. http://dx.doi.org/10.1038/35075138

Jongbloed, S.L., A.J. Kassianos, K.J. McDonald, G.J. Clark, X. Ju, C.E. Angel, C.J. Chen, P.R. Dunbar, R.B. Wadley, V. Jeet, et al. 2010. Human CD141+ (BDCA-3)+ dendritic cells (DCs) represent a unique myeloid DC subset that cross-presents necrotic cell antigens. *J. Exp. Med.* 207:1247–1260. http://dx.doi.org/10.1084/jem.20092140

Kautz-Neu, K., M. Noordegraaf, S. Dinges, C.L. Bennett, D. John, B.E. Clausen, and E. von Stebut. 2011. Langerhans cells are negative regulators of the anti-*Leishmania* response. *J. Exp. Med.* 208:885–891. http://dx.doi.org/10.1084/jem.20102318

Klechevsky, E. 2013. Human dendritic cells - stars in the skin. *Eur. J. Immunol.* 43:3147–3155. http://dx.doi.org/10.1002/eji.201343790

Klechevsky, E., R. Morita, M. Liu, Y. Cao, S. Coquery, L. Thompson-Snipes, F. Briere, D. Chaussabel, G. Zurawski, A.K. Palucka, et al. 2008. Functional specializations of human epidermal Langerhans cells and CD14+ dermal dendritic cells. *Immunity*. 29:497–510. http://dx.doi.org/10.1016/j.immuni.2008.07.013

Klechevsky, E., M. Liu, R. Morita, R. Banchereau, L. Thompson-Snipes, A.K. Palucka, H. Ueno, and J. Banchereau. 2009. Understanding human myeloid dendritic cell subsets for the rational design of novel vaccines. *Hum. Immunol.* 70:281–288. http://dx.doi.org/10.1016/j.humimm.2009.02.004

Langfelder, P., and S. Horvath. 2008. WGCNA: an R package for weighted correlation network analysis. *BMC Bioinformatics*. 9:559. http://dx.doi.org/10.1186/1471-2105-9-559

Lenz, A., M. Heine, G. Schuler, and N. Romani. 1993. Human and murine dermis contain dendritic cells. Isolation by means of a novel method and phenotypical and functional characterization. *J. Clin. Invest.* 92:2587–2596. http://dx.doi.org/10.1172/JCI116873

Liard, C., S. Munier, A. Joulin-Giet, O. Bonduelle, S. Hadam, D. Duffy, A. Vogt, B. Verrier, and B. Combadière. 2012. Intradermal immunization triggers epidermal Langerhans cell mobilization required for CD8 T-cell immune responses. *J. Invest. Dermatol.* 132:615–625. http://dx.doi.org/10.1038/jid.2011.346

Matthews, L., G. Gopinath, M. Gillespie, M. Caudy, D. Croft, B. de Bono, P. Garapati, J. Hemish, H. Hermjakob, B. Jassal, et al. 2009. Reactome knowledgebase of human biological pathways and processes. *Nucleic Acids Res.* 37(Database):D619–D622. http://dx.doi.org/10.1093/nar/gkn863

Meredith, M.M., K. Liu, G. Darrasse-Jeze, A.O. Kamphorst, H.A. Schreiber, P. Guermonprez, J. Idoyaga, C. Cheong, K.H. Yao, R.E. Niec, and M.C. Nussenzweig. 2012. Expression of the zinc finger transcription factor zDC (Zbtb46, Btbd4) defines the classical dendritic cell lineage. *J. Exp. Med.* 209:1153–1165. http://dx.doi.org/10.1084/jem.20112675

Miller, J.C., B.D. Brown, T. Shay, E.L. Gautier, V. Jojic, A. Cohain, G. Pandey, M. Leboeuf, K.G. Elpek, J. Helft, et al. Immunological Genome Consortium. 2012. Deciphering the transcriptional network of the dendritic cell lineage. *Nat. Immunol.* 13:888–899. http://dx.doi.org/10.1038/ni.2370

Nagao, K., F. Ginhoux, W.W. Leitner, S. Motegi, C.L. Bennett, B.E. Clausen, M. Merad, and M.C. Udey. 2009. Murine epidermal Langerhans cells and langerin-expressing dermal dendritic cells are unrelated and exhibit distinct functions. *Proc. Natl. Acad. Sci. USA*. 106:3312-3317. http://dx.doi.org/10.1073/pnas.0807126106

Nestle, F.O., X.G. Zheng, C.B. Thompson, L.A. Turka, and B.J. Nickoloff. 1993. Characterization of dermal dendritic cells obtained from normal human skin reveals phenotypic and functionally distinctive subsets. *J. Immunol.* 151:6535–6545.

Ng, S.Y., T. Yoshida, J. Zhang, and K. Georgopoulos. 2009. Genome-wide lineage-specific transcriptional networks underscore Ikaros-dependent lymphoid priming in hematopoietic stem cells. *Immunity*. 30:493–507. http://dx.doi.org/10.1016/j.immuni.2009.01.014

Novershtern, N., A. Subramanian, L.N. Lawton, R.H. Mak, W.N. Haining, M.E. McConkey, N. Habib, N. Yosef, C.Y. Chang, T. Shay, et al. 2011. Densely interconnected transcriptional circuits control cell states in human hematopoiesis. *Cell.* 144:296–309. http://dx.doi.org/10.1016/j.cell.2011.01.004

Polak, M.E., L. Newell, V.Y. Taraban, C. Pickard, E. Healy, P.S. Friedmann, A. Al-Shamkhani, and M.R. Ardern-Jones. 2012. CD70-CD27 interaction augments CD8+ T-cell activation by human epidermal Langerhans cells. *J. Invest. Dermatol.* 132:1636–1644. http://dx.doi.org/10.1038/jid.2012.26

Poulin, L.F., M. Salio, E. Griessinger, F. Anjos-Afonso, L. Craciun, J.L. Chen, A.M. Keller, O. Joffre, S. Zelenay, E. Nye, et al. 2010. Characterization of human DNGR-1+ BDCA3+ leukocytes as putative equivalents of mouse CD8alpha+ dendritic cells. *J. Exp. Med.* 207:1261–1271. http://dx.doi.org/10.1084/jem.20092618

Ratzinger, G., J. Baggers, M.A. de Cos, J. Yuan, T. Dao, J.L. Reagan, C. Münz, G. Heller, and J.W. Young. 2004. Mature human Langerhans cells derived from CD34+ hematopoietic progenitors stimulate greater cytolytic T lymphocyte activity in the absence of bioactive IL-12p70, by either single peptide presentation or cross-priming, than do dermal-interstitial or monocyte-derived dendritic cells. *J. Immunol.* 173:2780–2791. http://dx.doi.org/10.4049/jimmunol.173.4.2780

Romani, N., B.E. Clausen, and P. Stoitzner. 2010. Langerhans cells and more: langerin-expressing dendritic cell subsets in the skin. *Immunol. Rev.* 234:120–141. http://dx.doi.org/10.1111/j.0105-2896.2009.00886.x

Satpathy, A.T., W. Kc, J.C. Albring, B.T. Edelson, N.M. Kretzer, D. Bhattacharya, T.L. Murphy, and K.M. Murphy. 2012. Zbtb46 expression distinguishes classical dendritic cells and their committed progenitors from other immune lineages. *J. Exp. Med.* 209:1135–1152. http://dx.doi.org/10.1084/jem.20120030

Segura, E., and J.A. Villadangos. 2009. Antigen presentation by dendritic cells in vivo. *Curr. Opin. Immunol.* 21:105–110. http://dx.doi.org/10.1016/j.coi.2009.03.011

Segura, E., M. Durand, and S. Amigorena. 2013. Similar antigen cross-presentation capacity and phagocytic functions in all freshly isolated human lymphoid organ-resident dendritic cells. *J. Exp. Med.* 210:1035–1047. http://dx.doi.org/10.1084/jem.20121103

Seneschal, J., R.A. Clark, A. Gehad, C.M. Baecher-Allan, and T.S. Kupper. 2012. Human epidermal Langerhans cells maintain immune homeostasis in skin by activating skin resident regulatory T cells. *Immunity*. 36:873–884. http://dx.doi.org/10.1016/j.immuni.2012.03.018

Seré, K., J.H. Baek, J. Ober-Blöbaum, G. Müller-Newen, F. Tacke, Y. Yokota, M. Zenke, and T. Hieronymus. 2012. Two distinct types of Langerhans cells populate the skin during steady state and inflammation. *Immunity*. 37:905–916. http://dx.doi.org/10.1016/j.immuni.2012.07.019

Silberberg, I., R.L. Baer, and S.A. Rosenthal. 1976. The role of Langerhans cells in allergic contact hypersensitivity. A review of findings in man and guinea pigs. *J. Invest. Dermatol.* 66:210–217. http://dx.doi.org/10.1111/1523-1747.ep12482139

Sparber, F., C.H. Tripp, M. Hermann, N. Romani, and P. Stoitzner. 2010. Langerhans cells and dermal dendritic cells capture protein antigens in the skin: possible targets for vaccination through the skin. *Immunobiology*. 215:770–779. http://dx.doi.org/10.1016/j.imbio.2010.05.014

Subramanian, A., P. Tamayo, V.K. Mootha, S. Mukherjee, B.L. Ebert, M.A. Gillette, A. Paulovich, S.L. Pomeroy, T.R. Golub, E.S. Lander, and J.P. Mesirov. 2005. Gene set enrichment analysis: a knowledge-based approach for interpreting genome-wide expression profiles. *Proc. Natl. Acad. Sci. USA*. 102:15545–15550. http://dx.doi.org/10.1073/pnas.0506580102

Wang, Y., K.J. Szretter, W. Vermi, S. Gilfillan, C. Rossini, M. Cella, A.D. Barrow, M.S. Diamond, and M. Colonna. 2012. IL-34 is a tissue-restricted ligand of CSF1R required for the development of Langerhans cells and microglia. *Nat. Immunol.* 13:753–760. http://dx.doi.org/10.1038/ni.2360